INFLUENCE OF HEAT TREATMENT ON Al0.5Cr0.5Ni0.5TiZr1.5Nb1.5 HIGH ENTROPY ALLOY

Mihai Tudor OLARU[1], Mihail TARCOLEA[2], Dumitru MITRICA[1], Marian BURADA[1], Daniela DUMITRESCU[1], Cristina BANICA[1], Beatrice CARLAN[1]

High temperatures applications require special alloys caring superior properties that are stable at elevated temperatures. High entropy alloys are an emerging set of alloys mostly composed of a minimum of 5 or more elements in equimolar or non-equimolar ratio that develops outstanding properties such as mechanical strength, hardness, stiffness and corrosion resistance. Present work investigates the structure and properties of an as-cast and heat treated Al0.5Cr0.5Ni0.5TiZr1.5Nb1.5 high entropy alloy. The alloy specimens were cast by induction melting in Ar protective atmosphere, heat treated at 700÷1000°C for 10 hours and characterized by structural and mechanical techniques. Scanning electron microscopy analysis on as cast sample presents a homogenous dendritic structure well developed and distributed in the central area but underdeveloped on the side areas of the alloy. Heat treated sample reveals grains growth and higher structural homogeneity.

Key words: HEA, multicomponent, alloys, high, entropy, characterization, heat treatment

1. Introduction

High-entropy multicomponent alloys have attracted more attention due to their unique properties caused by simple crystalline structures despite multiple-component mixing. These type of alloys present attractive features such as high hardness, very good wear resistance, fatigue strength, good resistance to breakage at high temperatures, good thermal stability and increased resistance to oxidation and corrosion. High entropy alloys have hardening mechanisms based on solid solution strengthening, which are different from conventional alloys. Typically, high entropy alloys have high melting points and high yield resistance which can be maintained at very high temperatures. The properties of the alloys used for various applications depend largely on their composition. By the substitution of one or more elements in HEA composition, significant changes in properties can be obtained. Also, the decrease or increase in the quantity of the addition elements can lead to different structures with important influences on the properties of the

[1] National R&D Institute for Nonferrous and Rare Metals –IMNR, Pantelimon, Romania, corresponding author's e-mail: mihai.tudor.olaru@gmail.com
[2] Prof., Dept. of Metallic Materials Science, University POLITEHNICA of Bucharest, Romania

alloys [1].

There is a substantial amount of papers that describe the thermodynamics intricacies related to solid solution formation in high entropy alloys. Significant criteria were developed based on the mixing entropy, mixing enthalpy, atomic size difference, valence electron configuration and electronegativity of various high entropy alloy systems [2-4], which are contributing to the selection of viable alloy compositions for the different applications. Computer Aided Phase Prediction was also performed on various HEA systems, using specialized methods such as Calphad, Dendity Functional Theory, Monte Caro or Molecular Dynamics, with significant results in approximating phase constitution and evolution at different compositions and temperatures [29-34].

The effect of annealing on HEAs has been also studied suggesting that an aging AlCoCrFeNiTi alloy for 2h at 1000°C presents changes in microstructure and mechanical properties from the cast structure [35] Also, 4h annealing at varying temperatures on the hardness of an AlCrCuFeNiTi alloy was also investigated in literature [36].

Present paper is studying a high entropy alloy based on Al-Cr-Ni-Ti-Zr-Nb system taking into account the influence of different heat treatment temperatures on the alloy structure.

2. Materials and methods

Due to the large number of possible combinations of elements that can be used for HEA synthesis, several thermodynamic criteria that can be used for selection of HEA compositions with certain properties have been defined. Literature on thermodynamic criteria on high entropy alloys presents some aspects that can predict the formation of solid solutions in the alloy. Configurational entropy calculated with Boltzmann's formula ΔS_{conf} should be higher than 11 J/moleK and lower than 19.5 J/moleK; calculated mixing entropy ΔH_{mix} should have values between -11.6 kJ/mole and 3.2 kJ/mole [2]. Atomic radius size differences between the elements δ, which plays a major role on the formation of solid solutions should be less than 6.6% for promoting a majority of solid solutions in the alloy, and less than 4% for solid solutions formation exclusively [3]. Along with the atomic radius δ, Ω derivate parameter also define the formation of solid solutions being influenced by ΔS_{conf} and ΔH_{mix}. This parameter should only be considered next to δ. Electronegativity difference $\Delta\chi$ of the alloy components has to be between 3 and 6% (calculated with Allen values) [4]. The valence electron concentration (VEC) as a critical factor for establishing phase stability, points to the type of solid solution crystalline structure. An VEC smaller than 6.87 suggests the formation of BCC solid solutions, between 6.87 and 8 the alloy should develop BCC and FCC structures. If VEC is larger than 8, only FCC

solid solution structures are formed [5]. Another component of the whole criteria for HEA forming is k_1^{cr} factor, which indicates the presence or absence of intermetallic compounds. k_1^{cr} value should be higher than the ratio between ΔH_{IM} and ΔH_{mix}, in order to form only solid solutions [27, 28].

In this paper Al0.5Cr0.5Ni0.5TiZr1.5Nb1.5 high entropy alloy was calculated using criteria found in literature and obtained by melting and casting in induction melting furnace under argon inert atmosphere. The values of the evaluation parameters calculated for criteria of the microstructures for the experimental high entropy alloy using the combination of the elements Al, Cr, Ni, Ti, Zr, Nb is presented in table 1. Data for the calculation of ΔH_{mix} was acquired from Takeuchi and Inoue [6], atomic radius values of elements was taken from Senkov and Miracle [7]. Remaining parameters values were taken from [8, 9, 10, 26]. Phase equilibrium diagram of the studied alloy was obtained using MatCalc 6.02 thermodynamic modelling software containing CALPHAD data bases for a large spectrum of temperatures. Ni-based superalloy database was used for phase equilibrium calculation of Al0.5Cr0.5Ni0.5TiZr1.5Nb1.5 high entropy alloy. Melting and casting process started with pure raw aluminium, chromium, nickel, titanium, zirconium and niobium raw materials that were ultrasound cleaned in isopropyl alcohol for 10 minutes and dried in air. The dried chunks of cleaned metals were loaded inside induction furnace alumina crucible. The melting process started at a pressure of 0.6 mbar and reached a temperature of 1900°C. The ingot resulted from the casting was cooled down to room temperature in a cylindrical shaped copper mold and sliced in disk-shaped equal pieces. Resulted samples were heat treated in furnace at different temperatures for 10 hours inside Nabertherm 04/17 heat treatment furnace under argon atmosphere.

Chemical composition of the resulted sample was analyses by optical emission spectrometry in inductively coupled plasma (ICP-OES) using an Agilent 725 spectrometer. Scanning electronic microscopy and EDS mapping was performed using FEI Quanta 250 electronic microscope on previously etched samples. The etching solution was a mixture of 1 to 3 cc HF, 4 cc HNO_3, 100 cc H_2O solution to enhance the visibility of the grains and the grain boundaries.

The crystalline structure was analysed by X-ray diffractometry (XRD). Data acquisition was performed on BrukerD8ADVANCE diffractometer using Bruker DIFFRACPlus software, Bragg–Brentano diffraction method, H–H coupled in vertical configuration, with the following parameters: Cu Ka radiation, 2H region: 2041240, 2H step: 0.020, time/step: 8.7 s/step. Cu Kb radiation was removed with SOL X detector. Resulted data was processed using Bruker DIFFRACPlus EVA v12 software to search the database ICDD powder diffraction file (PDF-2, 2006 edition) and the full pattern matching (FPM) module of the same software package. FPM is a global fitting of the measured scan with a simulated scan. FPM

allows the identification of average crystallite size and refinement of lattice parameters.

3. Results and discussion

Criteria prediction calculations showed that the alloy composition is characterized by the high entropy effect, with ΔS_{conf} value higher than 11 J/moleK. Atomic size difference of 8.1% and ΔH_{mix} of -20 suggests that the alloy will contain moderate to high amounts of intermetallic compounds. The type of solid solutions that will form in the alloy is given by the valence electron concentration (VEC) which suggest a BCC structure is expected to form. The ration between ΔH_{IM} and ΔH_{mix} is higher than K_1^{cr} factor which indicates that not only solid solution will form.

Table 1

Calculated parameters for microstructural criteria prediction

Alloy	ΔS_{conf}, J/mole K	ΔH_{mix} kJ/mole	δ, %	VEC, %	Δχ (Allen) %	Ω	K_1^{cr}	$\Delta H_{IM}/\Delta H_{mix}$
Al0.5Cr0.5Ni0.5TiZr1.5Nb1.5	13.90	-20	8.1	4.9	9.78	1.4	1.27	1.31

Thermodynamic modelling results of the Al0.5Cr0.5Ni0.5TiZr1.5Nb1.5 alloy are presented in fig. 1-2. Variation of niobium in the alloy mix (fig 1 a) presents the formation multiple phases at different contents. Under 10 wt% Nb the alloy should have a A3 with HCP structure and a Laves phase. The addition of Nb above 10 wt% enhances the formation of Delta phase and slightly reduces the Laves phase. Continuing the addition of Nb above 27 wt%, the amount of Laves and Delta phases starts to drastically decrease but a new BCC structured A2 phase starts to form. Thermodynamic modelling of Zr content in the alloy (fig. 1b) suggests the formation of the BCC structured A2 phase also above 27 wt% and a decrease in Delta and Laves phase in further addition.

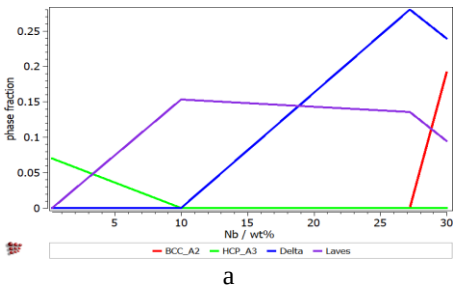

a

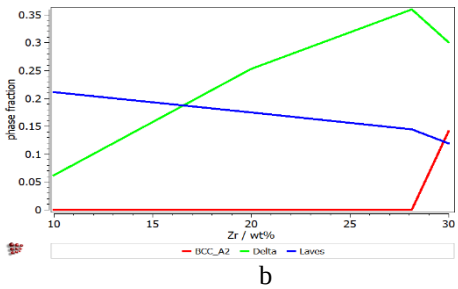

b

Fig. 1 Influence of Nb (a) and Zr (b) content on phase diagram of Al0.5Cr0.5NixTiZr1.5Nb1.5 high entropy alloy calculated using MatCalc

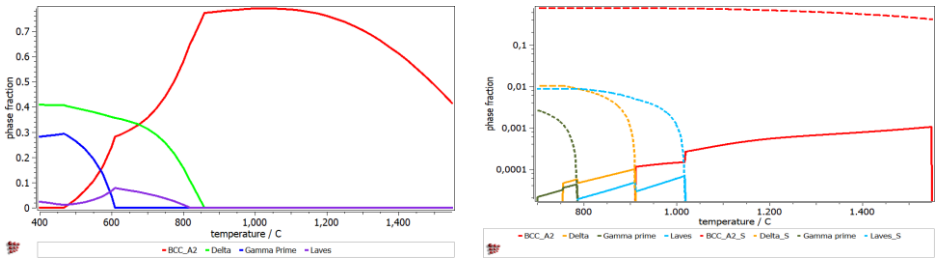

a b

Fig. 2 Phase equilibrum diagram (a) and Scheil-Gulliver solidification diagram (b) of Al0.5Cr0.5Ni0.5TiZr1.5Nb1.5 high entropy alloy calculated using MatCalc. Dotted line represents non-equilibrium phases, full line represents equilibrium phase

Phase equilibrum diagram shows couples of critical temperatures. At 600ºC the formation of Gamma Prime phase is inhibited, at 800ºC the small content of Laves phase is also inhibited along with Delta phase at aproximately 850ºC. BCC structured A2 solid solution phase is present in the alloy starting with 470ºC. With temperature increase, the A2 phase gains propotions transforming the alloy in a single-phased alloy at 1000ºC.

In fig. 2 b Sheil-Gulliver solidification diagram is presented. It can be observed that at high temperatures the non-equilibrium phase A2 is strongly formed. At 1000ºC Laves phases starts to form followed by Delta and Gamma Prime phases. At 830ºC the content of Laves phase and Delta phase are equal in proportions comparing with the equilibrium phase diagram (fig.2 a) where is cleary showed that Delta phase is higher in proportion than Laves.

The chemical composition was analysed by ICP-OES and revealed similar content of elements with slight differences in the cast alloy compared to the nominal composition. The results of the chemical analysis are presented in table 2.

Table 2

Chemical composition of the resulted sample

Alloy	Chemical composition, in mass %					
	Al	Cr	Nb	Zr	Ti	Ni
Nominal	3.43	6.61	35.46	34.82	12.18	7.46
As-cast	4.36	6.92	34.30	33.70	13.00	7.50

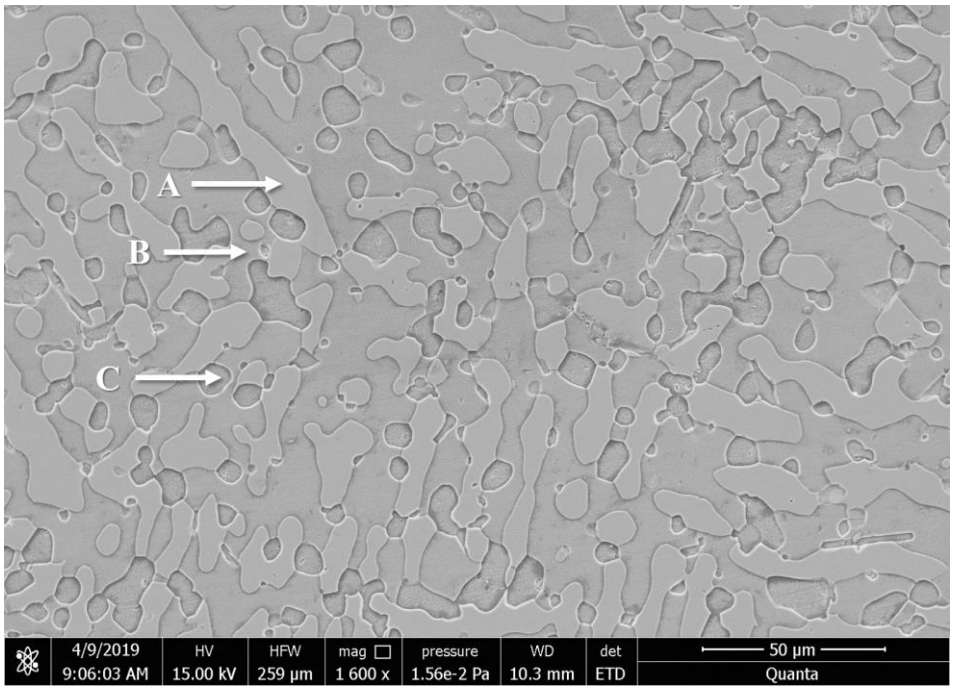

Fig. 3 As-cast alloy sample

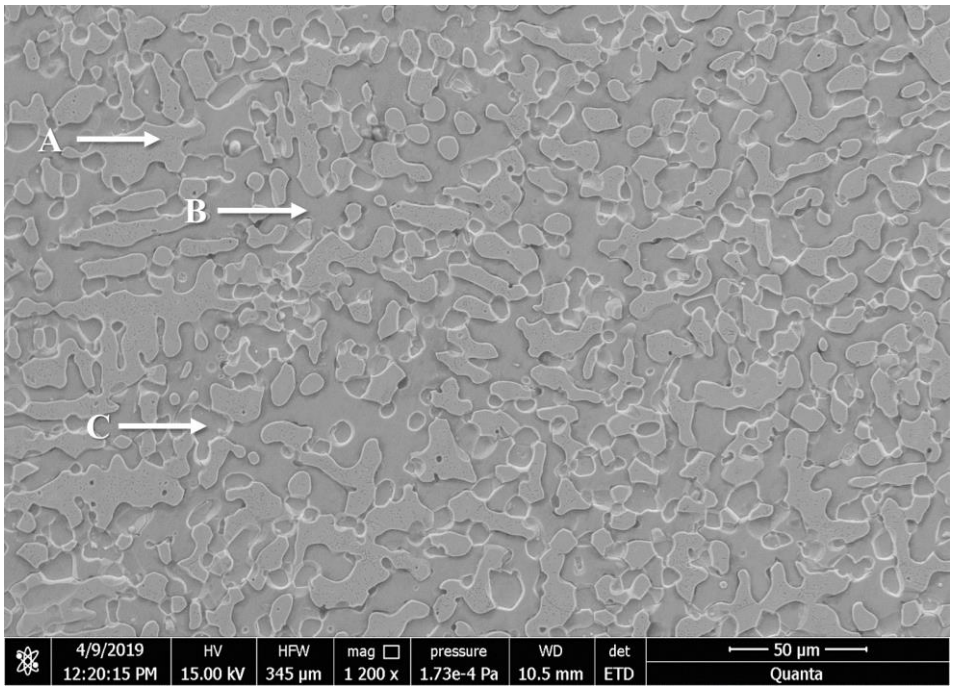

Fig. 4 Heat treated at 700°C sample

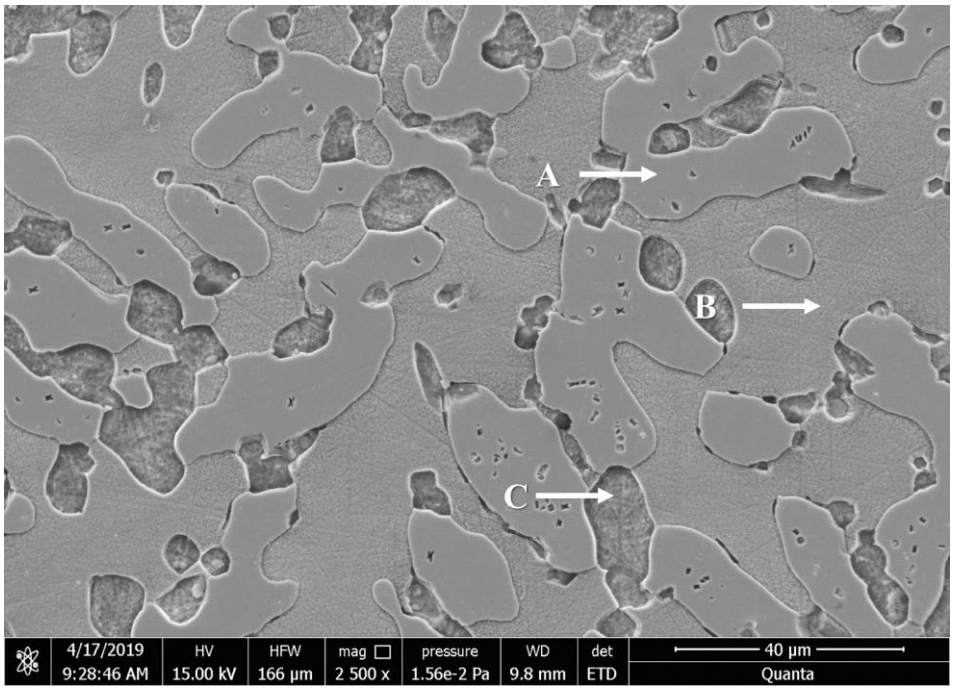

Fig. 5 Heat treated at 900°C sample

The morphology of the as-cast and heat-treated alloy samples was analysed by scanning electronic microscopy. SEM analysis of the as-cast sample (fig. 3) indicates the presences of three main phases: the dendritic zone phase (A) and inter-dendritic zone consisting of phases (B) and (C). (A) phase is composed of lengthen dendrites with small secondary arms. The dendrites have irregular shapes and do not have symmetrical orientation. (B) and (C) phases forms the inter-dendritic zone, (B) is the larger inter-dendritic phase uniformly spread in the alloy mass. (C) phase is shown as small round shaped islands in the (B) phase. Figs. 4-6 presents the morphology of the heat-treated samples at 700, 900 and 1000°C. It can be observed that after 700ºC heat-treatment process the microstructure shows a smaller dendritic area (A) but with similar configuration as as-cast sample (fig. 4). The (C) phase zones presents smaller islands areas but with greater density. After 900ºC heat-treatment the alloy presents unfinished phase transformations in part of the sample where larger dendrites are presents with greater (B) phase amounts (fig. 5). This suggests the action of the slow diffusion process specific to high entropy alloys and the necessity of a longer heat-treatment time in order to satisfy the diffusion process. Also, it can be observed that (C) phase is present in larger quantities in the sample. After 1000°C heat-treatment process the alloy sample presents a compact structure with less amount of (C) phase (fig. 6).

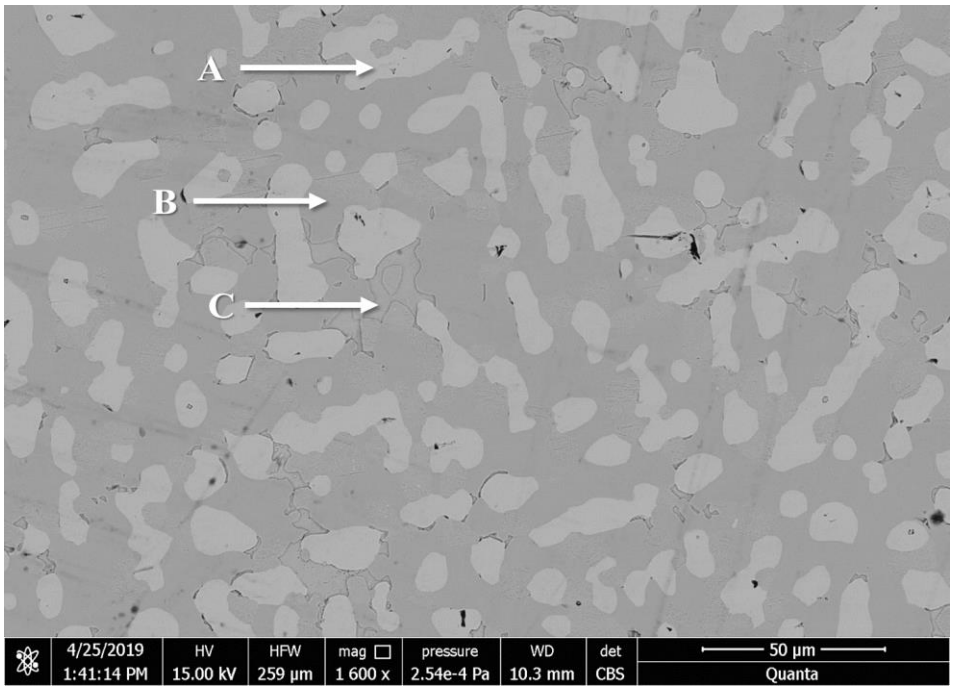

Fig. 6 Heat-treated at 1000°C sample, CBS image.

Figs. 7-10 presents EDS analysis of the as-cast and heat-treated samples. In the as-cast sample EDS mapping image, the elements are distributed majorly in the (B) phase zones where high quantities of aluminium, zirconium and chromium along with small amounts of nickel and titanium are present. The dendritic (A) phase is composed of high quantities of niobium and titanium but the island shaped (C) phase composition is mostly zirconium. After the heat-treatment processes the elemental composition of the all three phases is not affected with the exception of chromium which can be found in slightly more quantities in the (B) phase after the 1000℃ heat-treatment. Also, after the last heat-treatment the zirconium segregations can be found more often.

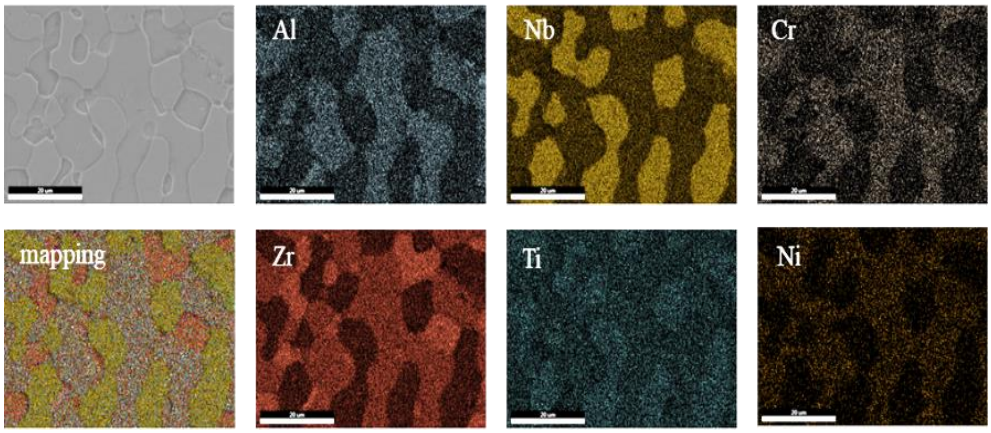

Fig. 7 EDS mapping analysis on as-cast HEA sample.

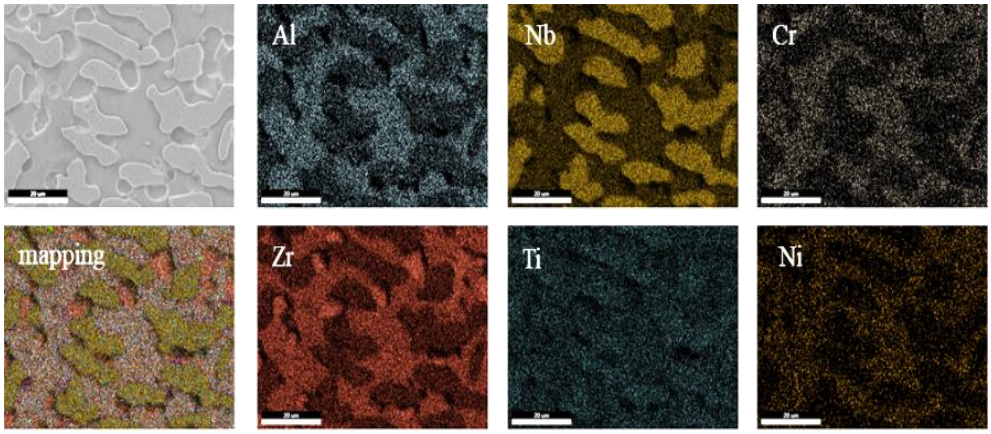

Fig. 8 EDS mapping analysis of 700°C heat treated HEA sample.

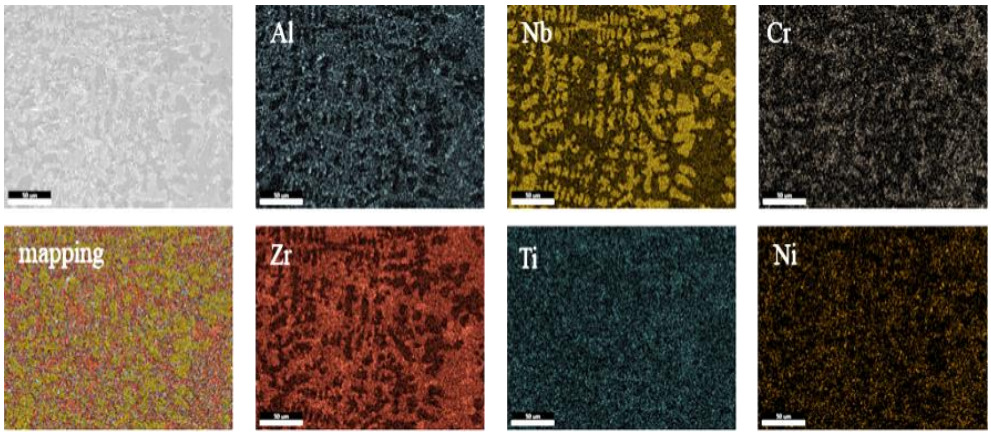

Fig. 9 EDS mapping analysis of 900°C heat treated HEA sample.

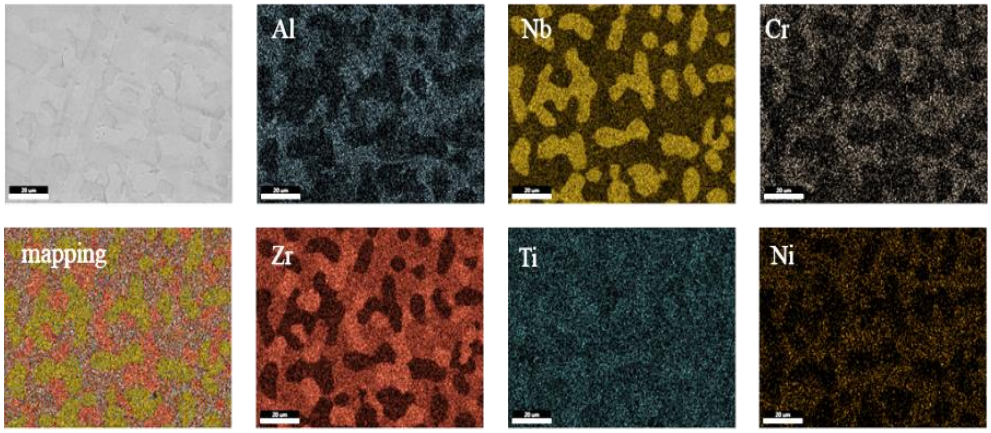

Fig. 10 EDS mapping analysis of 1000°C heat treated HEA sample.

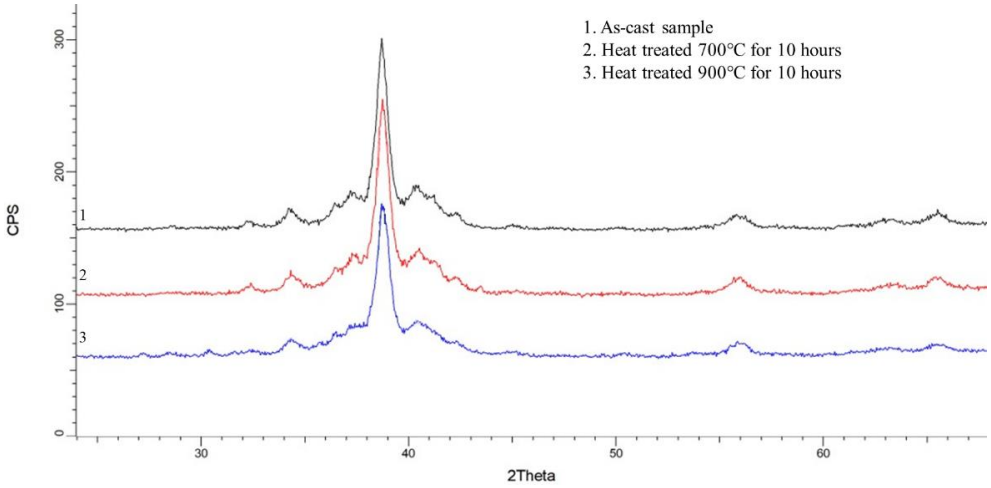

Fig. 11 XRD spectrum on as-cast and heat treated HEA samples

Crystalline structure of the as-cast and heat-treated samples are presented in fig. 11 and detailed in table 3. As-cast sample is composed of 3 solid solutions, two cubic phases and one with hexagonal structure. A2 is a body centred cubic disordered type of structure generated by Al-Cr rich precipitate. C14 is hexagonal type Laves solid solution phase rich in Zr, Ti and Cr, D8a is a body centred cubic Delta solid solution phase. Comparing with the EDS, SEM and XRD of the as-cast and heat-treated alloy samples, one can assume A2 phase is represented by the A zones on the SEM images, D8a is represented by the B inter-dendritic large phase rich in Al, Ni and Zr and C14 is represented by the Zr rich zones noted as C [37]. After the heat-treatment at different temperatures, samples present changes in phase proportions. A2 phase zones are getting smaller with each heat-treatment.

Also, C14 rich in Zr phase is also losing proportions. Instead, the D8a inter-dendritic phase is gathering amounts.

Table 3

Phases contained in HEA samples resulted from XRD spectrum analysis

Sample	Compound Name	S-Q ms.%	Lattice parameter, Å	System Space Group
1 As-Cast	Ss type A2	48	a 3.289	Cubic
	Ss type C14	30	a 5.233 c 8.538	Hexagonal
	Ss type D8a	22	a 12.073	Cubic
2 HT 700°C	Ss type A2	46	a 3.289	Cubic
	Ss type D8a	29	a 12.073	Cubic
	Ss type C14	25	a 5.233 c 8.538	Hexagonal
3 HT 900°C	Ss type A2	44	a 3.289	Cubic
	Ss type D8a	33	a 12.073	Cubic
	Ss type C14	23	a 5.233 c 8.538	Hexagonal

4. Conclusions

The chemical and microstructural analysis of as-cast alloy show high homogeneity across the samples and dendritic structures of relatively small dimensions. The three phases are evenly distributed in the alloy mass. After SEM, EDS and XRD analysis the three phases are considered to be solid solution phases, two cubic and one with hexagonal structure. The dendritic phase is rich in niobium and titanium, the inter-dendritic phase is mainly formed of Al, Cr, Ni and Zr and the third phase is a rich in Zr precipitate. Heat-treatment changes the phases proportions due to the slow diffusion typically to high entropy alloys. The rich in Zr precipitate loses proportion due to the diffusion on Zr in D8a inter-dendritic zone. Phase diagram obtained by MatCalc modelling of the Al0.5Cr0.5Ni0.5TiZr1.5Nb1.5 high entropy alloys is in partial accordance with the obtained alloy, three from four phases indicated by MatCalc modelling are present in the cast alloy. MatCalc modelling of Zr and Nb influence on the alloy structure is in accordance with the XRD results of the cast alloy, all the indicated phases are present in the cast alloy.

Acknowledgments

This work was supported by research grants of the Romanian National Authority for Scientific Research and Innovation, CNCS/CCCDI – UEFISCDI, project numbers: COFUND-M-ERA.NET II – 75/2017 HEAMODELL (1) and 20 PCCDI/2018, within PNCDI III.

R E F E R E N C E S

[1]. *J. W Yeh.*, High entropy multielement alloys, US patent 0159914A1, 2002.
[2]. *A. Takeuchi, A. Inoue*, Calculations of mixing enthalpy and mismatch entropy for ternary amorphous alloys, Materials Transactions Japan Institute Metals, vol. 41, 2000, pp. 1372–1378.
[3]. *Y. Zhang, Y. J. Zhou, J. P. Lin, G. L. Chen and P. K. Liaw*, Solid-solution phase formation rules for multi-component alloys, Advanced Engineering Materials, vol. 10, 2008, pp. 534–538.
[4]. *M. G. Poletti, L. Battezzati*, Electronic and thermodynamic criteria for the occurrence of high entropy alloys in metallic systems, Acta Materialia, vol. 75, 2014, pp. 297–306.
[5]. *S. Guo, C. Ng, J. Lu, C. T. Liu*, Effect of valence electron concentration on stability of fcc or bcc phase in high entropy alloys, Journal of Applied Physics, vol. 109, 2011, pp. 1–5.
[6]. *A. Takeuchi, A. Inoue*, Metallic glasses by atomic size difference, heat of mixing and period of constituent elements and its application to characterization of the main alloying element, Materials Transactions, vol. 46, 2005, pp. 2817–2829.
[7]. *O. N. Senkov, D. B. Miracle*, Effect of the atomic size distribution on glass forming ability of amorphous metallic alloys, Materials Research Bulletin, vol. 36, 2001, pp. 2183–2198.
[8]. *J. B. Mann, T. L. Meek, L. C. Allen*, Configuration energies of the main group elements, Journal of the American Chemical Society, vol. 122, 2000, pp. 2780–2783.
[9]. *J. B. Mann, T. L. Meek, E. T. Knight, J. F. Capitani, L. C. Allen*, Configuration energies of the d-block elements, Journal of the American Chemical Society, vol. 122, 2000, pp. 5132–5137.
[10]. *S. Guo, C. T. Liu*, Phase stability in high entropy alloys: Formation of solid-solution phase or amorphous phase, Progress in Natural Science: Materials International, vol. 21, 2011, pp. 433–446.
[11]. *J.-W. Yeh, S.-K. Chen, S.-J. Lin, J.-Y. Gan, T.-S. Chin, T.-T. Shun, C.-H. Tsau, S.-Y. Chang*, Nanostructured high-entropy alloys with multiple principal elements: novel alloy design concepts and outcomes, Advanced Engineering Materials, vol. 6, no. 5, 2004, pp. 299-303
[12]. *J.-W. Yeh*, Alloy Design Strategies and Future Trends in High-Entropy Alloys, JOM, vol 65, no 12, 2013, pp. 1759–1771.
[13]. *B.S. Murty Jien-Wei Yeh S. Ranganathan P. P. Bhattacharjee*, High-entropy alloys, second edition, Elsevier, 2019.
[14]. *Z. Wang, S. Guo, C. T. Liu*, Phase Selection in High-Entropy Alloys: From Nonequilibrium to Equilibrium, JOM, vol 66, issue 10, 2014, pp. 1966–1972.
[15]. *Alonso, J.A., Simozar, S.*, Prediction of solid solubility in alloys, Physical Review B, vol. 22, 1980, pp. 5582-5589.

[16]. *Ashby M.F.*,Materials: a brief history, Philosophical Magazine Letters. 88, 2008, pp. 749-755.
[17]. *Bhattacharjee, P.P., Sathiaraj, G.D., Zaid, M., Gatti, J.R., Lee, C., Tsai, C.W.*,. Microstructure and texture evolution during annealing of equiatomic CoCrFeMnNi high-entropy alloy. Journal of Alloys and Compounds, vol. 587, 2014, pp. 544-552.
[18]. *Cahn, R.W.*, The Coming of Materials Science, Elsevier Science Ltd., Amsterdam 2001.
[19]. *Cantor, B., Chang, I.T.H., Knight, P., Vincent, A.J.B.*, Microstructural development in equiatomic multicomponent alloy, Materials Science and Engineering: A vol. 375-377, 2004, pp. 213-218.
[20]. *Jien-Wei Yeh and Su-Jien Lin*, Breakthrough applications of high-entropy materials, Journal of Materials Research Society, vol. 33, 2018, pp. 3129-3137.
[21]. *Emil Babic, Damir Pajic, Krešo Zadro, Katica Biljakovic, Vesna Mikšic Trontl, Petar Pervan, Damir Starešinic, Ignacio A. Figueroa, Ahmed Kuršumovic, Štefan Michalik, Andrea Lachová, György Remenyi, Ramir Ristic*, Structure property relationship in (TiZrNbCu)1−xNix metallic glasses, Journal of Materials Research, vol. 33, 2018, pp. 3170-3183.
[22]. *Zhiming Li, Alfred Ludwig, Alan Savan, Hauke Springer and Dierk Raabe*, Combinatorial metallurgical synthesis and processing of high-entropy alloys, Journal of Materials Research Society, vol. 33, 2018, pp.3156-3169.
[23]. *Oleg N. Senkov, Daniel B. Miracle and Kevin J. Chaput*, Development and exploration of refractory high entropy alloys, Journal of Materials Research Society vol. 33, 2018, pp. 3092-3128.
[24]. *Mengdi Zhang and Lijun Zhang, Peter K. Liawb, Gong Lia, Riping Liu*, Effect of Nb content on thermal stability, mechanical and corrosion behaviors of hypoeutectic CoCrFeNiNb high-entropy alloys, Journal of Materials Research Society, vol.33, 2018, pp. 3276-3286.
[25]. *Vishal Sonib, Bharat Gwalanib, Oleg N. Senkov, Babu Viswanathan, Talukder Alam, Daniel B. Miracle, Rajarshi Banerjeea*, Phase stability as a function of temperature in a refractory highentropy alloy, Journal of Materials Research Society, vol. 33, 2018, pp.3235-3246.
[26]. https://www.webelements.com/periodicity/melting_point/
[27]. *M. Claudia Troparevsky, James R. Morris, Paul R. C. Kent, Andrew R. Lupini, G. Malcom Stocks*, Criteria for predicting the formation of single-phase high-entropy alloys, Physical Review X, vol. 5, 2015,
[28]. *O.N. Senkov, D.B. Miracle*, A new thermodynamic parameter to predict formation of solid solution or intermetallic phases in high entropy alloys, Journal of Alloys and Compounds, vol. 658, 2016.
[29]. *Zhang C. Zhang F. Chen S. Cao W*. Computational Thermodynamics Aided High-Entropy Alloy Design, JOM vol. 64, 2012, pp. 839–845.
[30]. *Zhang F. Zhang C. Chen S. L. Zhu J. Cao W. S. Kattner U. R.*, Calphad: Computer Coupling of Phase Diagrams and Thermochemistry, vol.45, 2014, pp. 1–10.
[31]. *Widom M. Huhn W. P. Maiti S. and Steurer W*. Hybrid Monte Carlo/Molecular Dynamics Simulation of a Refractory Metal High Entropy Alloy, Metallurgical and Materials Transactions A, vol. 45, 2014, pp. 196-20.

[32]. *Middleburgh S. C. King D. M. Lumpkin G. R. Cortie M. and Edwards L.*, Segregation and migration of species in the CrCoFeNi high entropy alloys, Journal of Alloys and Compounds, vol. 599, 2014, pp 179–182.
[33]. *Ma D. Grabowski B. Körmann F. Neugebauer J. and Raabe D.,* Ab initio thermodynamics of the COCrFeMnNi high entropy alloy: Importance of the entropy contributions beyond the configurational one, Acta Materialia, vol. 100, 2015, pp 90–97.
[34]. *Troparevsky M. C. Morris J. R. Daene M. Wang Y. Lupini A. R. and Stocks G. M.,* Beyond Atomic Sizes and Hume-Rothery Rules: Understanding and Predicting High-Entropy Alloys, JOM vol. 67, 2015, pp. 2350–2363.
[35]. *Zhang K.B., Fu Z.Y., Zhang J.Y., Shi J., Wang W.M., Wang H., Wang Y.C., Zhang Q.J.*, Annealing on the structure and properties evolution of the CoCrFeNiCuAl high-entropy alloy, Journal of Alloys and Compounds, vol. 502, 2010, pp. 295–299.
[36]. *Hsu U.S., Hung U.D., Yeh J.W., Chen S.K., Huang Y.S., Yang C.C.*, Alloying behavior of iron, gold and silver in AlCoCrCuNi-based equimolar high-entropy alloys, Materials Science and Engineering: A. Structural Materials: Properties, Microstructure and Processing, vol. 460, 2007, pp. 403–408.
[37]. https://crystdb.nims.go.jp/crystdb/.